

Influence of hole shape on the transmission and negative refractive index properties of metal-dielectric-metal metamaterial

ZHONG Min^{1,2}

(1. Department of Physics, Nanjing Normal University, Nanjing 210023, China;
2. Hezhou College, Hezhou 542899, China)

Abstract: The transmission, negative refractive index (NRI) and figure of merit (FOM) of metal-dielectric-metal (MDM) sandwiched metamaterial, which is perforated with different length of rectangular holes, are numerically studied. The low-frequency transmission peak and maximum transmission peaks of rectangular hole are red-shifted with the increasing of the length of holes. The NRI and the frequency bandwidth of NRI of the rectangular holes are reduced with the increase of the length of holes. It becomes possible to obtain a higher transmission or NRI of metamaterial by adjusting the length of the rectangular holes on MDM metamaterial arrays.

Key words: metamaterial, negative refractive index, transmission, FOM

PACS: 41.20.Jb, 78.20.Cj, 73.20.Mf, 42.25.Bs

孔型对金属-介质-金属三明治结构超材料的透射率和负折射率的影响

钟敏^{1,2}

(1. 物理与科学技术学院 南京师范大学, 江苏 南京 210023;
2. 贺州学院, 广西 贺州 542899)

摘要: 通过改变长方形孔的长度, 利用数值模拟研究了金属-介质-金属三明治结构超材料的透射率, 负折射率 (NRI) 率和品质因数 (FOM) 等性质. 研究表明, 随着长方形孔的长度的增大, 低频透射峰和最大透射峰都出现了红移现象. 长方形孔的负折射率和负折射带宽则随着长方形孔的长度的增大而减小. 这意味着可以通过调节金属-介质-金属三明治结构超材料的孔阵列的长度获得较高的透射率或者负折射率. 这些结果为开发太赫兹范围的光电器件提供可能的理论.

关键词: 超材料; 负折射率; 透射率; FOM

中图分类号: O431 **文献标识码:** A

Introduction

Over the past decade, extraordinary optical transmission (EOT) and negative refractive index (NRI) of 2D hole arrays of sandwiched metamaterial are widely investigated because of their remarkable properties^[1-2]. Transmission properties of two dimensional (2D) hole arrays perforated in metamaterial of subwavelength apertures has become a very active research area in electromagnetism since EOT was reported by Ebbesen *et al*^[1]. The phenomenon was suggested to be associated with sur-

face plasmon polariton (SPP)^[2], composite diffracted evanescent wave^[3] and the excited surface electromagnetic Bloch wave on the metal surface^[4]. The influence of hole on the optical transmission properties of 2D hole arrays have been studied in many experiments^[5]. Moreover, the phase difference between the localized surface wave and the propagating surface Bloch wave can be adjusted through changing the geometrical parameters of the array with ring-shaped subwavelength apertures^[6]. Some studies indicate that the transmission properties of metamaterial with double sets of square holes is dependent on geometric parameters of the subwavelength holes and the

Received date: 2013 - 09 - 20, **revised date:** 2014 - 02 - 19

收稿日期: 2013 - 09 - 20, **修回日期:** 2014 - 02 - 19

Foundation items: Supported by National Natural Science Foundation of China (60778041), Graduate Research and Innovation Program of ordinary university of Jiangsu (CXLX13_390), Hezhou college scientific research projects (2011ZRKY06 and 2012ZRKY04)

Biography: Zhong Min(1982-), man, Hezhou, lecturer. Research area involves metamaterial, nano-optics, statistical physics. E-mail: zhongmin2012hy@163.com.

EOT phenomenon can be clearly illustrated for all of samples^[7]. It can be found in these experimental studies that transmission through a rectangular hole presents strong polarization dependencies and higher transmittance than circular or square holes with the same area and transmission resonances can be supported by a single rectangular hole. These studies only focus on the influence of hole shape on the transmission properties of one-dimensional array^[3-5]. The NRI and the frequency bandwidth of NRI of 2D hole arrays of sandwiched metamaterial were not considered in these studies. It is valuable to study the effect of hole shape on the transmittance and NRI properties of multi-layer structure metamaterial. In order to have a deeper insight into the influence of length of hole on properties of transmission and NRI of MDM sandwiched metamaterial, the transmission spectra and the negative refractive spectra are studied with the changing of the length of rectangular hole.

1 Model and method

A unit cell of our model under study is showed in Fig. 1 (a); a rectangular hole with the geometry of $a = 6 \mu\text{m}$ and $b = 2 \mu\text{m}$. The scanning electron microscopy (SEM) images of the sample are shown in Fig. 1 (b). The periodicity in the x-y plane is $P = 12 \mu\text{m}$. The lattice consists of three layers of media, two layers of silver and one layer of SU-8, respectively. The thickness of the silver film and the SU-8 layer are $s = 0.05 \mu\text{m}$ and $h = 2 \mu\text{m}$, respectively. In the simulation, we utilize two ideal magnetic conductor planes on the boundary normal to the x axis and two ideal electric conductor planes on the boundary normal to the y axis^[8]. The whole model is tested in air with light incident from air to the structure propagating along the z axis.

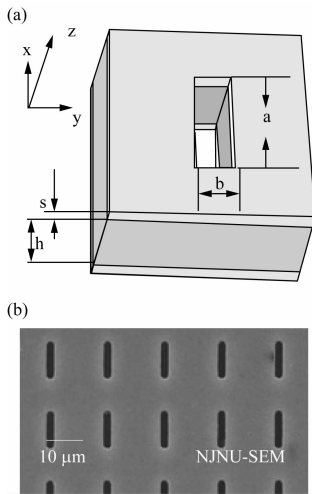


Fig. 1 Schematic of one unit cell and scanning electron microscopy image of sample

图1 设计的单元结构图以及样品 SEM 影像

The commercial software Ansoft HFSS13 has been used to perform the simulation. In the simulation, the dielectric constant of SU-8 is assumed to be $2.56 + 0.035i$ ^[9]. The silver layer is obtained using the Drude model:

$$\varepsilon(\omega) = 1 - \frac{\omega_p^2}{\omega^2 - i\omega\gamma_D}, \quad (1)$$

where $\gamma_D = 9 \times 10^{13} \text{ s}^{-1}$ is the collision frequency, $\omega_p = 1.37 \times 10^{16} \text{ s}^{-1}$ is the plasma frequency^[10]. The transmittance, negative refractive index and S parameters can be obtained for the unit cell^[11].

2 Results and discussion

The transmission spectra of simulated and measured results are showed in Fig. 2.

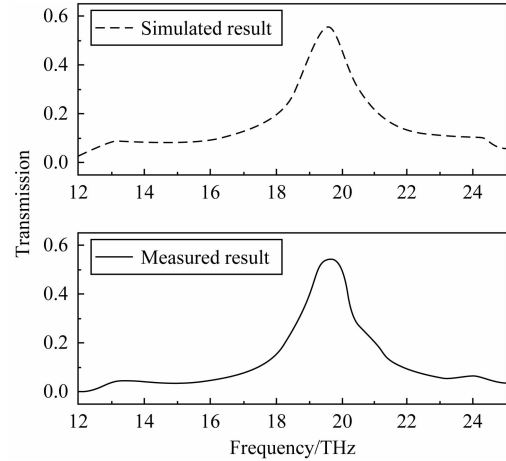


Fig. 2 The transmission spectra of simulated and measured results
图2 模拟透射率谱和测量透射率谱

It can be found that there are three transmission peaks in the mid-infrared region, one low-frequency transmission peak and two high-frequency transmission peaks. These high-frequency transmission peaks come from external surface plasmon polaritons (SPPs) and the low-frequency transmission peak comes from the internal SPPs^[12]. The good agreement between measured and simulated results in Fig. 2 verifies that our simulated results are valid. Moreover, there exists negative refractive index around the low-frequency transmission peak according to some studies^[2]. In order to have a deeper insight into the influence of the length of hole on properties of transmission and NRI of sandwiched metamaterial, the hole in Fig. 1 (a) is changed to $6 \mu\text{m} \times 2 \mu\text{m}$, $7 \mu\text{m} \times 2 \mu\text{m}$, $8 \mu\text{m} \times 2 \mu\text{m}$ and $9 \mu\text{m} \times 2 \mu\text{m}$, with other parameters kept unchanged.

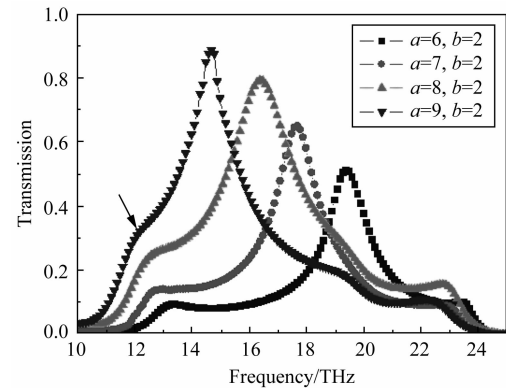


Fig. 3 Transmission spectra with different length $a = 6 \mu\text{m}$, $7 \mu\text{m}$, $8 \mu\text{m}$ and $9 \mu\text{m}$

图3 不同长度的透射率谱

We calculate the transmission spectra corresponding to the length $a = 6 \mu\text{m}$, $7 \mu\text{m}$, $8 \mu\text{m}$, $9 \mu\text{m}$. As shown in Fig. 3 that maximum transmission peaks are 0.51 ($6 \mu\text{m} \times 2 \mu\text{m}$), 0.65 ($7 \mu\text{m} \times 2 \mu\text{m}$), 0.79 ($8 \mu\text{m} \times 2 \mu\text{m}$), 0.89 ($9 \mu\text{m} \times 2 \mu\text{m}$), respectively. The transmission spectrum of the sample with $9 \mu\text{m} \times 2 \mu\text{m}$ is obviously bigger than other samples. It can be found that maximum transmission peaks are red-shifted with the length increasing, as shown in Table 1.

Table 1 Maximum transmission and frequency of peak with different length $a = 6 \mu\text{m}$, $7 \mu\text{m}$, $8 \mu\text{m}$ and $9 \mu\text{m}$

表 1 不同长度的最大透射率和峰位

Length	$a = 6$	$a = 7$	$a = 8$	$a = 9$
Transmission	0.51	0.65	0.79	0.89
Position	19.4	17.7	16.4	14.7

Meanwhile the low-frequency transmission peak becomes less clear, indicated by the arrow in Fig. 3. We used Origin 8.0 software for numerical fitting to obtain a linear formula:

$$y = a + b * x \quad , \quad (2)$$

In Eq. 2, x indicates length and y indicates maximum transmission. The result of fitting is the red line as showed in Fig. 4, with the intercept $a = -0.25$ and the slope $b = 0.128$.

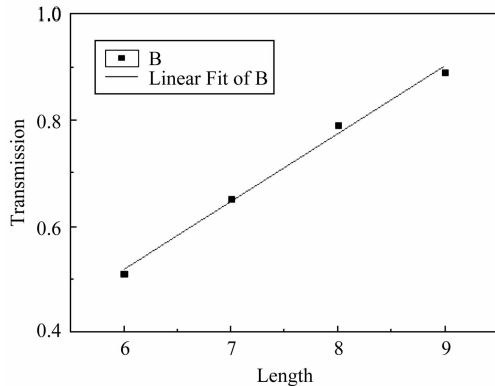


Fig. 4 The transmission spectra with different length $a = 6 \mu\text{m}$, $7 \mu\text{m}$, $8 \mu\text{m}$ and $9 \mu\text{m}$. The red line is the numerical fitting results
图 4 不同长度的透射率峰值关系谱, 红色线为数值模拟结果

Equation 2 indicates that the variation of maximum transmission with the length of hole follows a linear law. It means that an appropriate length of rectangular hole can be chosen to obtain the desired transmission.

It also can be found that low-frequency transmission peaks are red-shifted with the length increasing too. Values and center frequency of transmission peaks are sensitive to the length of hole. Refractive index of these sub-wavelength holes is showed in Fig. 5.

As shown in Fig. 5 that all of holes exhibits an NRI phenomenon. The NRI and the frequency bandwidth of NRI are -0.85 and 3.2 Thz ($a = 6 \mu\text{m}$), -0.82 and 3.3 Thz ($a = 7 \mu\text{m}$), -0.81 and 1.9 Thz ($a = 8 \mu\text{m}$), -0.55 and 1.4 Thz ($a = 9 \mu\text{m}$), respectively. It is obviously that all of negative refractive peaks are red-shifted. By comparing, we can find that the NRI and the frequency bandwidth of NRI of hole are reduced with the increase of the length of holes, as shown in Table 2. It

indicates that you can adjust the length of the rectangular hole to change the NRI and the frequency bandwidth of NRI.

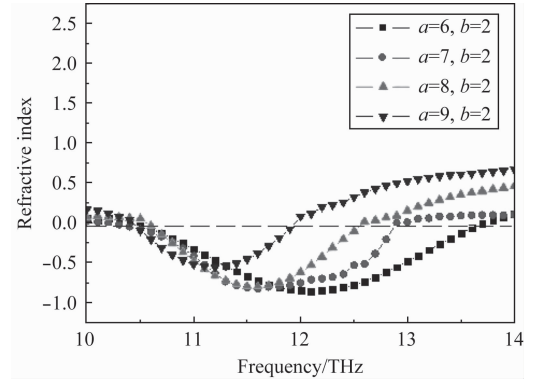


Fig. 5 Refractive index spectra with different length $a = 6 \mu\text{m}$, $7 \mu\text{m}$, $8 \mu\text{m}$ and $9 \mu\text{m}$

图 5 不同长度的折射率

Table 2 NRI and bandwidth of NRI for holes with different length $a = 6 \mu\text{m}$, $7 \mu\text{m}$, $8 \mu\text{m}$ and $9 \mu\text{m}$

表 2 不同长度孔洞的负折射率和负折射带宽

Length	$a = 6$	$a = 7$	$a = 8$	$a = 9$
NRI	-0.85	-0.82	-0.81	-0.55
Bandwidth	3.12	2.54	1.73	1.11

By comparing Fig. 3 with Fig. 5, the NRI and the frequency bandwidth of NRI are reduced with the length increasing. In order to find out the physics behind the reducing NRI and the frequency bandwidth of NRI as a function of the length of holes, the permittivity is retrieved from the simulated spectra of Fig. 3 and shown in Fig. 6. We see that bands of NRI coincide with these peaks of permittivity. It can be found that there exists negative permittivity around the low-frequency transmission peak which lead to the NRI, as shown by the arrow in Fig. 6. The NRI and the frequency bandwidth of NRI are reduced with the permittivity closing to zero.

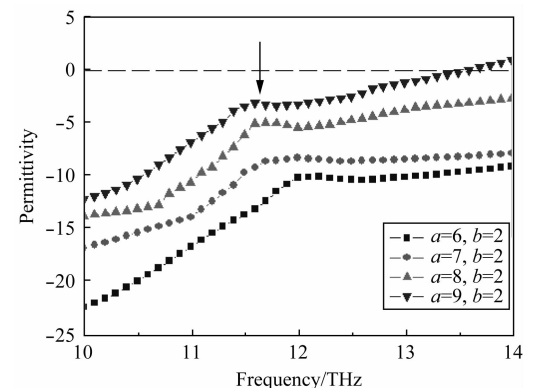


Fig. 6 Permittivity for holes with different length, $a = 6 \mu\text{m}$, $7 \mu\text{m}$, $8 \mu\text{m}$ and $9 \mu\text{m}$

图 6 不同长度的磁导率谱

We calculate the loss of MDM sandwiched metamaterials for electromagnetic waves with figure of merit (FOM):

$$\text{FOM} = -\text{Re}(n)/\text{Im}(n) \quad , \quad (3)$$

In the above formula, $\text{Re}(n)$ is the real part of the refractive index and $\text{Im}(n)$ is the imaginary part of the refractive index. The higher value of FOM, the lower loss of MDM sandwiched metamaterial is for electromagnetic wave. FOMs spectra corresponding to the length $a = 6 \mu\text{m}$, $7 \mu\text{m}$, $8 \mu\text{m}$ and $9 \mu\text{m}$ are shown in Fig. 7. FOMs increased at first, and then decreased. It means that there is an optimum length, at which the maximum FOM can be obtained.

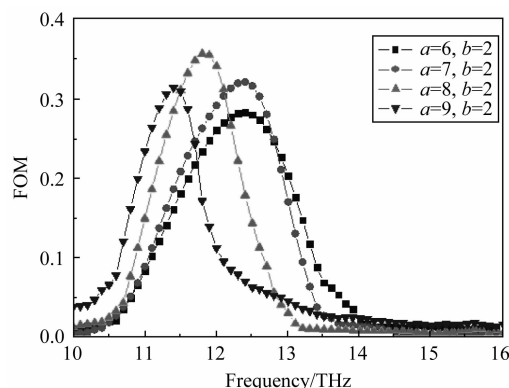


Fig. 7 FOM spectra for holes with different length $a = 6 \mu\text{m}$, $7 \mu\text{m}$, $8 \mu\text{m}$ and $9 \mu\text{m}$

图7 不同长度的FOM谱

3 Conclusions

Transmission, NRI and FOM of MDM sandwiched metamaterial perforated with different length of holes were numerically studied under the same conditions. Results suggest that center frequency of low-frequency transmission peaks and maximum transmission peaks are red-shifted with the increase of the length of holes. The NRI and the frequency bandwidth of NRI are reduced with the increasing of the length of the hole. The FOM of rectangular hole does not increase with the increase of the length. The variation of maximum transmission with the length of the hole follows a linear law. The study can enrich the possibility to control the transmission and NRI properties of MDM sandwiched metamaterial via changing

the geometric parameters of rectangular holes arrays. We can obtain a higher transmission or NRI of metamaterial by adjusting the length of the rectangular hole on MDM metamaterial arrays.

References

- [1] Ebbesen T W, Lezec H J, Ghaemmi H F, *et al.* Extraordinary optical transmission through sub-wavelength hole arrays [J]. *Nature (London)*, 1998, **391**: 667 – 670.
- [2] Ortuno R, Garcia-Meca C, Rodriguez-Fortuno F J, *et al.* Role of surface plasmon polaritons on optical transmission through double layer metallic hole arrays [J]. *Phys. Rev. B*, 2009, **79**: 075425 – 075435.
- [3] Gay G, Alloschery O, Viaris de Lesegno B, *et al.* The optical response of nanostructured surfaces and the composite diffracted evanescent wave model [J]. *Nature physics*. 2006, **2**: 262 – 267.
- [4] Martín-Moreno L, García-Vidal F J, Lezec H J, *et al.* Theory of Extraordinary Optical Transmission through Subwavelength Hole Arrays [J]. *Phys. Rev. Lett.* 2001, **86**: 1114 – 1117.
- [5] Gordon R, Brolo A G, Mckinnon A, *et al.* Strong polarization in the optical transmission through elliptical nanohole arrays [J]. *Phys. Rev. Lett.* 2004, **92**: 037401 – 037404.
- [6] Bao Y J, Peng R W, Shu D J, *et al.* Role of Interference between Localized and Propagating Surface Waves on the Extraordinary Optical Transmission Through a Subwavelength-Aperture Array, *Phys. Rev. Lett.* 2008, **101**: 087401 – 087404.
- [7] Zou S, Liu J S, Wand K J. Microwave transmission properties of metamaterials with double sets of square holes [J]. *Chinese Science Bulletin*, 2012, **57**: 3769 – 3772.
- [8] Smith D R, Schultz S, Markos P, *et al.* Determination of effective permittivity and permeability of metamaterials from reflection and transmission coefficients [J]. *Phys. Rev. B*. 2002, **65**: 195104 – 195108.
- [9] Hua Y L, Li Z Y. Analytic modal solution to transmission and collimation of light by one-dimensional nanostructured subwavelength metallic slits [J]. *J. Appl. Phys.* 2009, **105**: 013104 – 013111.
- [10] Smith D R, Vier D C, Kongschny T, *et al.* Electromagnetic parameter retrieval from inhomogeneous metamaterials [J], *Phys. Rev. E*. **71**: 036617 (2005).
- [11] Zhang S, Fan W J, Paniou N C, *et al.* Experimental Demonstration of Near-infrared Negative-Index Metamaterials [J]. *Phys. Rev. Lett.* 2005, **95**: 137404 – 137407.
- [12] Wang X D, Ye Y H, Ma J, *et al.* Influence of Filling Medium of Holes on the Negative-Index Response of Sandwiched Metamaterials [J]. *Chin. Phys. Lett.* 2010, **27**: 094101 – 094103.